JBIC Journal of Biological Inorganic Chemistry (2021) 26:1–11
https://doi.org/10.1007/s00775-020-01832-w

ORIGINAL PAPER

Effective binding of Tb^{3+} and La^{3+} cations on the donor side of Mn-depleted photosystem II

Elena R. Lovyagina[1] · Aleksey V. Loktyushkin[1] · Boris K. Semin[1]

Received: 8 June 2020 / Accepted: 20 October 2020 / Published online: 4 November 2020

Abstract

The interaction of Tb^{3+} and La^{3+} cations with different photosystem II (PSII) membranes (intact PSII, Ca-depleted PSII (PSII[-Ca]) and Mn-depleted PSII (PSII[-Mn]) membranes) was studied. Although both lanthanide cations (Ln^{3+}) interact only with Ca^{2+}-binding site of oxygen-evolving complex (OEC) in PSII and PSII(-Ca) membranes, we found that in PSII(-Mn) membranes both Ln^{3+} ions tightly bind to another site localized on the oxidizing side of PSII. Binding of Ln^{3+} cations to this site is not protected by Ca^{2+} and is accompanied by very effective inhibition of Mn^{2+} oxidation at the high-affinity (HA) Mn-binding site ([Mn^{2+} + H_2O_2] couple was used as a donor of electrons). The values of the constant for inhibition of electron transport K_i are equal to 2.10 ± 0.03 μM for Tb^{3+} and 8.3 ± 0.4 μM for La^{3+}, whereas OEC inhibition constant in the native PSII membranes is 323 ± 7 μM for Tb^{3+}. The value of K_i for Tb^{3+} corresponds to K_i for Mn^{2+} cations in the reaction of diphenylcarbazide oxidation via HA site (1.5 μM) presented in the literature. Our results suggest that Ln^{3+} cations bind to the HA Mn-binding site in PSII(-Mn) membranes like Mn^{2+} or Fe^{2+} cations. Taking into account the fact that Mn^{2+} and Fe^{2+} cations bind to the HA site as trivalent cations after light-induced oxidation and the fact that Mn cation bound to the HA site (Mn4) is also in trivalent state, we can suggest that valency may be important for the interaction of Ln^{3+} with the HA site.

Keywords Photosystem II · Oxygen-evolving complex · Calcium · Terbium · Lanthanum · High-affinity Mn-binding site

Abbreviations

Chl	Chlorophyll
DCBQ	2,6-Dichloro-*p*-benzoquinone
DCPIP	2,6-Dichlorophenolindophenol
DPC	Diphenylcarbazide
HA	High-affinity Mn-binding site
MES	2-(*N*-Morpholino)-ethanesulfonic acid
Ln^{3+}	Lanthanide ions
OEC	Oxygen-evolving complex
PSII	Photosystem II
PSII(-Ca)	Ca^{2+}-depleted PSII membranes
PSII(-Mn)	Mn-depleted PSII membranes
RC	Reaction center
Tris	Tris(hydroxymethyl)aminomethane

Electronic supplementary material The online version of this article (https://doi.org/10.1007/s00775-020-01832-w) contains supplementary material, which is available to authorized users.

✉ Boris K. Semin
semin@biophys.msu.ru

[1] Department of Biophysics, Faculty of Biology, Moscow State University, Moscow 119234, Russia

Introduction

The light absorbed by plants, algae, and cyanobacteria is used by these organisms for water decomposition. This process is carried out by the multicomponent membrane pigment–protein complex called photosystem II (PSII). Water oxidation reaction in PSII supplies electrons to the photosynthetic electron transport chain, triggering the synthesis of high-energy components. The remaining oxygen atoms are a by-product of this reaction. Therefore, the catalytic center oxidizing water [water splitting or oxygen evolving complex (OEC)] carries out the synthesis of an intermolecular bond between two oxygen atoms of two water molecules. Synthetized oxygen is released into the atmosphere and this photosynthetic reaction is practically the only source of O_2 in the atmosphere of our planet. The catalytic center of the OEC consists of four manganese cations, one calcium cation, and five oxygen atoms connecting the metal cations [1–3]. The detailed structure of a catalytic cluster Mn_4CaO_5 has been determined at first by X-ray diffraction at 1.9 Å resolution [1] and then with using femtosecond X-ray pulses at 1.95 Å resolution [3]. The latter method allowed to obtain a 'radiation-damage-free' structure of Mn/Ca cluster. In subsequent

works, a comparative study of the structure of the PSII cores in the dark state (S1) and S3 state (after two flashes) was carried out [4]. The effect of Mn_4CaO_5 cluster extraction from OEC on the PSII structure was also investigated [5]. Currently, not only is the structure of the PSII core determined, but also more complex formations—the supercomplex of the PSII core with the light-harvesting complex II [6]. The results obtained made it possible to establish that the cluster is coordinated by one imidazole and six carboxyl groups of amino acid residues of the D1 and CP43 proteins of PSII and have four molecules of water, two of which are bound to Mn4 cation and the other two cations bound to Ca^{2+} cation. The cluster has an irregular cube structure formed by three manganese cations and a Ca^{2+} cation connected via oxygen bridges. The fourth manganese cation (Mn4) is connected to the cube by two oxygen bridges. However, despite the high resolution of the Mn_4CaO_5 structure decryption, the mechanism of the water-splitting reaction in PSII remains mostly unclear.

Ca^{2+} is a necessary cofactor for the water oxidation reaction [7]. A possible role of Ca^{2+} in this reaction is either "adjustment" of the redox potential of a manganese cluster [8, 9] or binding of one or two substrate water molecules that are oxidized during a catalytic cycle [10]. However, the specific mechanism of Ca^{2+} participation in the OEC functioning remains unclear [8]. The role of Ca^{2+} in the water splitting mechanism was investigated in many works with the use of substitution of calcium cation with another metal cation. Ca^{2+} binding is competitive with divalent cations such as Cd^{2+} [11], Sr^{2+} [12], the only metal ion which partially functionally replaces Ca^{2+}, and lanthanides [13, 14]. The substitution of Ca^{2+} by lanthanide ion (denoted as Ln^{3+}) has proven to be an effective method for investigating the properties of different Ca^{2+}-binding proteins since ions are very effective competitive inhibitors of the Ca^{2+} site [15]. Various lanthanides were used for studying the Ca-binding site in the OEC of intact PSII [13], Ca-depleted PSII membranes (PSII(-Ca)) [14] and PSII core complexes [16]. Though all lanthanides show very similar chemical properties, significant differences in the action of specific ions on the PSII functioning [14] were revealed. These variations are probably caused by different ion radius. Displacement of Ca^{2+} by La^{3+} inhibits the oxygen evolution in intact PSII, preventing the electron donation by Mn cations to Y_Z [13]. The presence of lanthanides also affects the electron transfer from Y_Z to $P680^+$ [17]. A lanthanide-substituted OEC displayed a thermoluminescence band arising from S_2Q_A charge recombination, indicating that the Mn cluster is oxidized to the S_2 state [14]. EPR studies of Dy^{3+}-substituted PSII also have shown the S1 → S2 transition [16].

Ghanotakis et al. mentioned in their work [13] dedicated to a research of La^{3+} interaction with Ca-binding site in the OEC of native PSII membranes that Ce^{3+} and Tb^{3+} produce the same effect as La^{3+}. In a preliminary study [18], we have investigated the effect of terbium, one of the poorly studied lanthanides, on the native PSII membranes using the fluorescence method. In this paper, we investigated in detail the interaction of Tb^{3+} (and La^{3+} for comparison) with different PSII membranes (intact PSII, PSII(-Ca) and Mn-depleted PSII membranes (PSII(-Mn)). Although both Ln^{3+} cations interact only with Ca^{2+} site of the OEC in PSII and PSII(-Ca) membranes, we found that in PSII(-Mn) membranes both lanthanide ions tightly bind to another site localized on the oxidizing side and inhibiting very effectively ($K_i = 2.10 \pm 0.03$ μM for Tb^{3+} and 8.3 ± 0.4 μM for La^{3+}) the donation of electrons by ($Mn^{2+} + H_2O_2$) donor via the high-affinity (HA) Mn-binding site in these membranes.

Materials and methods

PSII preparations

Native PSII membranes PSII-enriched membrane fragments (BBY-type) were prepared from market spinach following Ghanotakis and Babcock [19]. The functional and spectral characteristics of these preparations matched the previously reported one [20]. Table S1 of Supplementary Material section shows some characteristics of intact PSII membranes as well as PSII(-Ca) and PSII(-Mn) membranes which were determined mainly in our previous works. Some parameters were measured in several different studies with good agreement with each other. This indicates a fairly good uniformity of the PSII samples we prepare. The preparations were stored at − 80 °C in buffer A, containing 15 mM NaCl, 400 mM sucrose, and 50 mM MES/NaOH buffer (pH 6.5). Samples were thawed in the dark for 1 h at 0 °C before treatment or measurement. Chlorophyll concentrations were determined in 80% acetone, according to the method of Porra et al. [21].

Ca^{2+} depletion Calcium ions, PsbP, and PsbQ extrinsic proteins were removed from native PSII membranes together using a buffer solution containing 2 M NaCl, 0.4 M sucrose, and 25 mM MES (pH 6.5) [22]. The PSII preparations were incubated in this buffer at 0.5 mg/ml Chl for 15 min under room light (4–5 μE m^{-2} s^{-1}) and at room temperature (22 °C). The resulting material was washed twice with buffer A, and re-suspended in buffer A. This preparation is referred to as PSII(–Ca) membranes. We do not use the chelator (EDTA or EGTA) during Ca^{2+} extraction, since the chelator binds to the Mn cluster changing its EPR signal in S2 state [23] and functional activity of Mn cluster [24]. The addition of the chelator is not necessary for Ca^{2+} extraction, since the extraction occurs only due to the change of affinity of calcium cation to its binding site when PsbQ and PsbP proteins are extracted [23]. The evidence of Ca extraction

from OEC by 2 M NaCl is the inhibition of O_2 evolution (the remaining activity may be about 10%) and the restoration of oxygen-evolving function by exogenous Ca^{2+} cations up to about 70% [24]. The absence of PsbP and PsbQ proteins in similar preparations obtained by us earlier was confirmed by polyacrylamide gel electrophoresis (see Table S1 in Supplementary Material). Mn content in Ca-depleted PSII membranes after NaCl treatment was 4.0 ± 0.2 Mn/RC.

Mn depletion by Tris treatment Manganese depletion was accomplished by incubating thawed PSII membranes (0.5 mg Chl/ml) in 0.8 M Tris–HCl buffer (pH 8.5) for 15 min in room light (4–5 μE m^{-2} s^{-1}) at room temperature. The membranes were then pelleted by centrifugation in an Eppendorf centrifuge 5415R (16100*g* × 3 min), washed three times with buffer A and finally re-suspended in buffer A. These membranes, which do not contain any extrinsic proteins (including PsbO polypeptide), Ca^{2+} ion, and the Mn catalytic cluster, are called PSII(–Mn) membranes. The absence of all extrinsic proteins in similar preparations obtained by us earlier was confirmed by polyacrylamide gel electrophoresis (see Table S1 in Supplementary Material). Residual Mn content in Mn-depleted PSII membranes after Tris treatment was 0.3 ± 0.1 Mn/RC.

PSII preparations activity

DCPIP reduction activity To determine electron transport activity we measured the rate of the exogenous electron acceptor 2,6-dichlorophenolindophenol (DCPIP) photoreduction. XBDROY light diodes (Cree Inc., USA) with the emission maximum of 450 nm providing a saturating light intensity (1500 μE m^{-2} s^{-1}) were used as the excitation light source. The reduction rate of DCPIP (40 μM) was determined spectrophotometrically from a change in the absorbance at 600 nm using the molar extinction coefficient for the deprotonated form of DCPIP (ε = 21.8 mM^{-1} cm^{-1} [25]). The electron transport activity of the native PSII membranes corresponds to 140–150 μmol DCPIP mg Chl^{-1} h^{-1}. The concentration of Chl in all samples was 20 μg/ml.

O_2-evolving activity Kinetics of a photoinduced oxygen evolution by PSII preparations were registered amperometrically using a closed Clark electrode. The measurements were carried out in a thermostatically controlled cell at 25 °C in the presence of 200 μM of an artificial electron acceptor 2,6-dichloro-*p*-benzoquinone (DCBQ). The oxygen evolution rate was calculated using a linear part of a kinetic curve for the first 10 s after the illumination was turned on. Calibration of a diffusion current magnitude was carried out using the value of the oxygen concentration in water balanced with air (253 μM). XBDROY light diodes were used as the excitation light source providing a saturating light intensity (1500 μE m^{-2} s^{-1}). The O_2-evolving activity of the native PSII membranes ranged from 450 to 550 μmol O_2 mg Chl^{-1} h^{-1}. The concentration of Chl in all samples was 10 μg/ml.

Fluorescence induction kinetics (FIK)

FIKs were measured using a portable Plant Efficiency Analyzer (Hansatech Instruments Ltd., UK). LED sources of excitation light (λ_{max} = 650 nm; spectral range 580–710 nm) were used in the fluorimeter. The time resolution of fluorescence detection was 10 μs (within the initial 2 ms); 1 ms (within the time interval from 2 ms to 1 s); and 100 ms (time interval > 1 s). Fluorescence induction kinetics were measured at actinic (1500 μE m^{-2} s^{-1}) intensity of the excitation light flux. The fluorescence signal at 50 μs after the application of continuous actinic light was defined as F_0. The initial moment of fluorescence detection in the figures corresponds to 50 μs. A logarithmic time scale was used in the figures as it is commonly employed for the presentation of fluorescence induction kinetics. Dark incubation before measurements was 2 min. The concentration of Chl in all samples was 20 μg/ml.

Determination of the Mn content in Ca-depleted PSII membranes

The Mn assays were performed according to the method of Semin and Seibert [26] with minor modifications [27]. The absorbance at 450 nm was used for colorimetric determination of Mn(II) concentrations using 3,3′,5,5′-tetramethylbenzidine as a chromogenic reagent (extinction coefficient of 34 mM^{-1} cm^{-1}) in the samples [28].

Metal ions treatment of PSII preparations

For the treatment of PSII preparation, we used the following salts: $La(CH_3COO)_3$; $Cr(NO_3)_3$; $AlCl_3$ dissolved in buffer A with control of pH; 5 мМ $Tb_2(SO_4)_3$ dissolved in buffer A. It should be noted that acetate ion and NO_3^- anions can inhibit the functional activity of PSII membranes, but in concentration significantly higher than that used in the present work [29, 30]. 50% inhibition of O_2-evolving activity is achieved at a concentration of 225 mM, and DCPIP reduction—650 mM sodium acetate [29].

Results and discussion

Interaction of Tb^{3+} and La^{3+} cations with PSII membranes

The lanthanides are very effective inhibitors of OEC in photosystem II and different Ln^{3+} cations were studied in several works [13, 14, 16, 31, 32]. Already in one of the

initial studies [13], it was found that La^{3+} ions inhibit OEC due to the substitution of Ca^{2+} for La^{3+}. These researchers have shown that La^{3+} competes with Ca^{2+} for binding site on the oxidizing side of PSII membranes. La^{3+} ion binds to the Ca-binding site more strongly than Ca^{2+} (the K_i for La^{3+} was estimated to be 0.05 mM compared to K_m for Ca^{2+} of 0.6 mM [13]). Further proof of this is the fact that external Ca^{2+} failed to reactivate PSII treated by Ln^{3+} [31]. However, bound Ln^{3+} ion can be removed using EDTA and oxygen-evolving activity can be reconstituted by adding back Ca^{2+} [31]. Most often La^{3+}, which has the ionic radius similar to the ionic radius of Ca^{2+} (1.17 Å and 1.14 Å respectively), was used in these investigations. Recently, we investigated the effect of Tb^{3+} ions with similar ionic radius (1.06 Å) [18] on the PSII OEC function. Terbium is one of the poorly studied lanthanides and in this study we probed terbium effects on the OEC by monitoring the fluorescence induction kinetic and oxygen evolution rate. Our results have shown that Tb^{3+} inhibits O_2 evolution at low concentration (50% inhibition is observed at concentration 0.5 mM) competing with Ca, since the addition of exogenous Ca^{2+} provided a significant protection of OEC against the inhibiting action of Tb^{3+} [18]. This result indicates that Tb^{3+} cation as well as La^{3+} [13] substitutes for Ca^{2+} cation in the OEC in the native PSII membranes.

In the above-mentioned works, the measurement of Ln^{3+} inhibition efficiency of PSII functional activity was carried out using O_2 evolution registration. Here, we investigated the effect of lanthanide ions on the electron transport rate in PSII, measuring the rate of DCPIP (artificial electron acceptor) reduction spectroscopically. It is necessary to note that these methods are not equivalent for measurement of electron transport in some PSII membranes. For example, in PSII(-Ca) membranes obtained by NaCl washing extraction of Ca^{2+} together with extrinsic proteins PsbP and PsbQ, O_2 evolving activity becomes about 10% from initial value whereas the rate of DCPIP reduction is about 70% [24]. Existence of rather intensive electron transport in PSII(-Ca) membranes is determined by water oxidation in the absence of Ca ion in the OEC not up to oxygen, but only up to H_2O_2 [33]. The obtained results are shown in Fig. 1 and demonstrate that La^{3+} is more active in the inhibition of O_2 evolution activity (concentration of 50% inhibition is 0.145 mM) than Tb^{3+} (concentration of 50% inhibition is 0.484 mM, $K_i = 323 \pm 7$ μM). Inhibition constants K_i were determined using Dixon analysis. Inhibition of DCPIP reduction reaction is observed at large concentrations of lanthanides: concentrations of 50% inhibition are equal 0.287 mM for La^{3+} and 1.21 mM for Tb^{3+} ($K_i = 454 \pm 9$ μM) (Fig. 1). It means that the replacement of Ca^{2+} in the OEC with Ln^{3+} inhibits more the reaction of O_2 synthesis than the reaction of water oxidation, i.e., calcium cation participates mainly on the last steps of the catalytic cycle in O_2 evolution process.

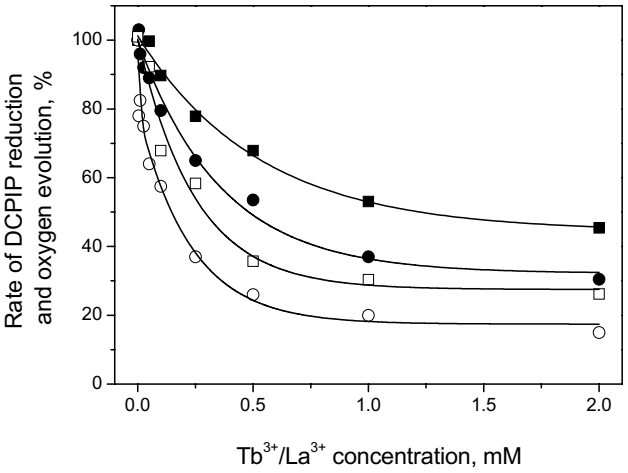

Fig. 1 Effect of Tb^{3+} (solid symbols) and La^{3+} (open symbols) on the oxygen evolution (circles) and DCPIP reduction (squares) in the native PSII membranes. The samples were incubated with Tb^{3+} or La^{3+} cations for 3 min at room temperature in the dark before measurements of O_2 evolution or DCPIP reduction. Concentration of PSII membranes in sample was 20 μg Chl/ml. 100% is the rate of O_2 evolution (450–550 μmol O_2 mg Chl^{-1} h^{-1}) or DCPIP reduction (150–180 μmol DCPIP mg Chl^{-1} h^{-1}) by native PSII membranes in buffer A

Thus, the inhibitory effect of La^{3+} cations on the oxygen-evolving activity of PSII membranes saturates at about 20% in the 0.7–2 mM region (concentration dependence on Fig. 1) at incubation time 3 min. The saturation level for Tb^{3+} is about 30% (1.3–2 mM region). We can suggest some versions of a hypothetical explanation for such character of inhibition concentration dependence with saturation at some level of oxygen release. First, Ca^{2+} depletion effectively inhibits the oxygen evolution [residual activity 10–25% (24 and references therein)]; however, the water oxidation reaction is inhibited significantly less [residual activity 70–75% (24 and references therein)]. Water is oxidized in such membranes to hydrogen peroxide. The generated H_2O_2 can split producing the molecular oxygen. Possibly, the OEC with Ln^{3+} cation instead of Ca^{2+} have increased catalase activity and residual O_2 concentration is determined by H_2O_2 splitting. Second, the concentration dependence of inhibition by Ln^{3+} cations' O_2 evolution indicates that in some part of PSII membranes, O_2 evolution reaction is not inhibited completely. It means that in some part of PSII samples, OEC is more resistant to the Ln^{3+} cation action, i.e., PSII preparations can be heterogenous. Heterogeneity of the OEC can be determined for example by the next reason. In the dark (during the treatment by Ln^{3+} cations), about 25% of the PSII complexes are in the S0 state, whereas the remaining 75% are in the S1 state. Extraction of Ca^{2+} cation from the OEC needs room light [22], i.e., Ca^{2+} is extracted better when the Mn cluster is in the higher S states. Therefore, we can suggest that the remaining O_2 evolution activity (≈20–30%)

after the treatment of PSII by Ln^{3+} is determined by slow extraction of Ca^{2+} from the S0 state (≈25%) of the OEC.

Interaction of Tb^{3+} cations with PSII(–Ca) membranes

Ca^{2+} cation can be efficiently extracted from the OEC by incubating the PSII membranes under light in a buffer supplemented with highly concentrated NaCl [22]. NaCl-treated PSII membranes lose extrinsic proteins PsbP and PsbQ as well as calcium ions from the OEC. The rate of O_2 evolution decreases to less than 10%, but can be restored by addition of Ca^{2+} ions to a concentration of about 10 mM. Another feature of PSII(–Ca) membranes is the availability of OEC for bulky reductants [34] and cations [34, 35], since the OEC is not protected by extrinsic proteins. The effect of different Ln^{3+} on the Ca^{2+}-depleted PSII membranes without 24 kDa extrinsic protein (their properties are similar to PSII(-Ca) membranes) was studied by Ono [14] and K_i values of these lanthanoids were determined. In our work, we investigated the effect of Tb^{3+} on the electron transfer in PSII(–Ca) membranes prepared by NaCl washing. Titration of Tb^{3+} effect is presented in Fig. 2. After incubation of samples with Tb^{3+}, the rate of oxygen evolution was measured in the presence of 10 mM Ca^{2+}. The curve with solid circles represents the concentration dependence of Tb^{3+} effect on the oxygen evolution. It shows that Tb^{3+} inhibits the electron transport in PSII(–Ca) membranes in the same concentration range as in native PSII membranes (compare Figs. 1 and 2). These data indicate that the Tb^{3+} cation inhibits the O_2 evolution due to tightly binding to the Ca-binding site and Ca^{2+} ion added after incubation of PSII(–Ca) membranes with Tb^{3+} cannot replace bound terbium cation. However, if Ca^{2+} cations were present during incubation of membranes with Tb^{3+}, the level of inhibition was significantly smaller (Fig. 2), i.e., Ca^{2+} ions prevent the interaction of Tb^{3+} ions with Ca site. The same results were obtained in the case of native PSII membranes: the presence of Ca^{2+} during La^{3+} treatment suppressed the inhibition of oxygen evolution [13]. This result shows that Tb^{3+} ions interact with the Ca-binding site of the OEC in the PSII(–Ca) membranes as in the native membranes. We calculated the inhibition constant for inhibition of electron transport in the PSII(–Ca) membranes by Tb^{3+} cations (K_i) using the Dixon plot (1/initial rate vs inhibitor concentration; [36]). The estimated K_i is equal to about 139 ± 5 µM. This value is similar to the K_i for inhibition of electron transport in Ca-depleted PSII membranes by La^{3+} (200 µM) [14].

Figure 3 shows the time-dependent change of O_2 evolution in PSII(–Ca) membranes during treatment with Tb^{3+} cations. Sample membranes at 0.25 mg Chl/ml were incubated in the dark with 1.0 mM Tb^{3+} in the presence of 30 mM Ca^{2+} (solid circles) or its absence (half open circles) for the indicated time at room temperature. O_2 evolution activity was measured in the presence of 10 mM Ca^{2+} after 50-fold dilution. Time dependence for Tb^{3+} is similar to the time dependence for La^{3+} determined by Ghanotakis et al. [13]. It is necessary to note that the protective effect of Ca^{2+}

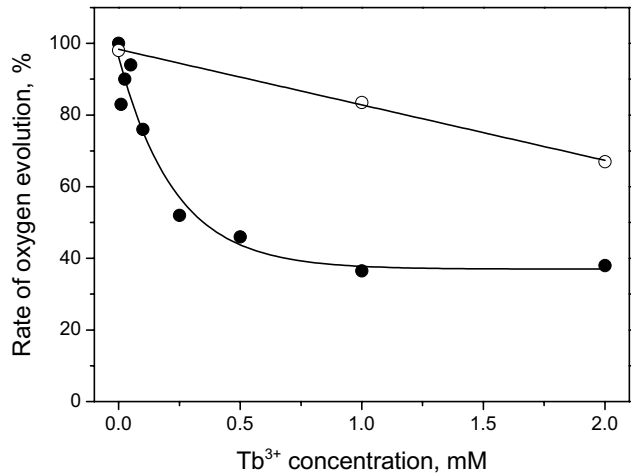

Fig. 2 Effect of Tb^{3+} (curve with solid circles) on the oxygen evolution in the PSII(-Ca) membranes. PSII(-Ca) membranes (10 µg Chl/ml) were incubated for 3 min at room temperature in the dark, in a buffer A and the indicated concentration of Tb^{3+} and then were assayed for oxygen evolution activity in the presence of 10 mM Ca^{2+} and 0.2 mM DCBQ (solid circles). The curve with open circles shows the Tb^{3+} effect on the oxygen evolving activity when 10 mM Ca^{2+} was included during terbium treatment. Control activity was 320–390 µmol O_2 mg Chl^{-1} h^{-1} in the presence of 10 mM Ca^{2+}

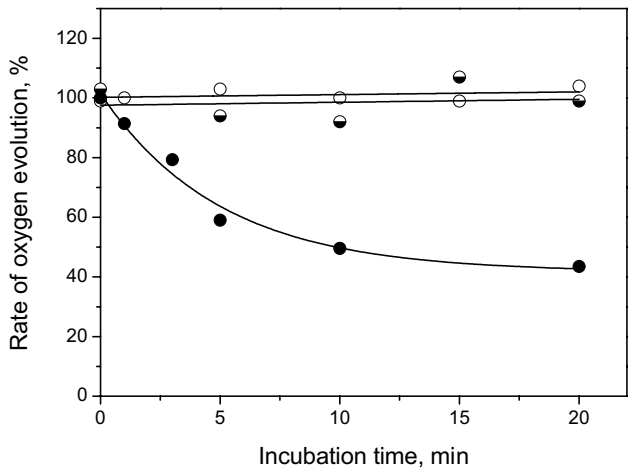

Fig. 3 The time course of Tb^{3+} cation interaction with Ca^{2+}-binding site in PSII(-Ca) membranes. Samples (0.25 mg Chl/ml) were incubated with 1 mM Tb^{3+} (solid circles), 1 mM Tb^{3+} plus 30 mM Ca^{2+} (half open circles) and no addition (open circles) for various times in the dark at room temperature. O_2 evolution activity was measured in the presence of 10 mM Ca^{2+} after 50-fold dilution of sample suspension. 100% activity represents 320–390 µmol O_2 mg Chl^{-1} h^{-1} for Ca-depleted PSII membranes in the presence of 10 mM Ca^{2+}.

in the time course experiment (Fig. 3) is more pronounced than in the results presented in Fig. 2 (concentration dependence). The possible reason for this can be a significant difference in the number of Tb^{3+} cations per reaction center (RC). This ratio is equal to 1000 in the time course experiment (Fig. 3) and 50,000 in the concentration experiment (Fig. 2). It means that in the experiment presented in Fig. 2, Tb^{3+} cations in large concentration can partially destroy the Mn cluster. The release of Mn from OEC during incubation of PSII membranes with La^{3+} was reported by Ghanotakis et al. [13].

Interaction of Tb^{3+} and La^{3+} cations with PSII(–Mn) membranes

PSII membranes treated with Tris at alkaline pH for OEC extraction have no Mn and Ca ions as well as all three extrinsic proteins and are not able to split water evolving the molecular oxygen. However, such membranes can oxidize exogenous electron donors under light and in the presence of exogenous electron acceptor like DCPIP and therefore the function of electron transport chain can be investigated. PSII(–Mn) membranes can be useful to study the localization of an inhibition site—is it OEC or, for example, the acceptor side of PSII. In the present work, we studied the effect of Tb^{3+} and La^{3+} ions on the electron transport chain in PSII(–Mn) membranes prepared by Tris treatment. Electron transport was supported by an exogenous electron donor ($Mn^{2+} + H_2O_2$). This electron donor donates electrons only via the HA Mn-binding site [37–40]. Electron transfer was probed by measurement of DCPIP reduction. Unexpectedly, we found that Tb^{3+} and La^{3+} ions inhibit DCPIP reduction supported by ($Mn^{2+} + H_2O_2$) electron donor at very small concentration (Fig. 4). The concentration of 50% inhibition is about 1 µM for Tb^{3+} ion (Fig. 4a) and about 3 µM for La^{3+} ion (Fig. 4b), compared with the concentrations of 50% OEC inhibition in the native PSII membranes—484 µM for Tb^{3+} and 145 µM for La^{3+} (Fig. 1). We calculated the inhibition constant for Tb^{3+} and La^{3+} cations inactivating electron transport supported by ($Mn^{2+} + H_2O_2$) donor in the PSII(–Mn) membranes using the Dixon plot. Estimated K_i values for inhibition of electron transport are equal to 2.10 ± 0.03 µM for Tb^{3+} and 8.3 ± 0.4 µM for La^{3+} (Fig. 5).

The effective inhibition of Mn^{2+} oxidation at the HA site by Tb^{3+} and La^{3+} cations is supported by the measurement of fluorescence induction kinetics (FIK) presented on Fig. 6a, b respectively. In native PSII samples, the FIK curve exhibits three characteristic points corresponding to F_0 (point O), the yield of fluorescence when Q_A is reduced (point J), and the F_{max} level (point P), where the plastoquinone pool (which quenches fluorescence in the oxidized form [41]) is also reduced. Extraction of the Mn cation from the OEC significantly changes the FIK curve, where

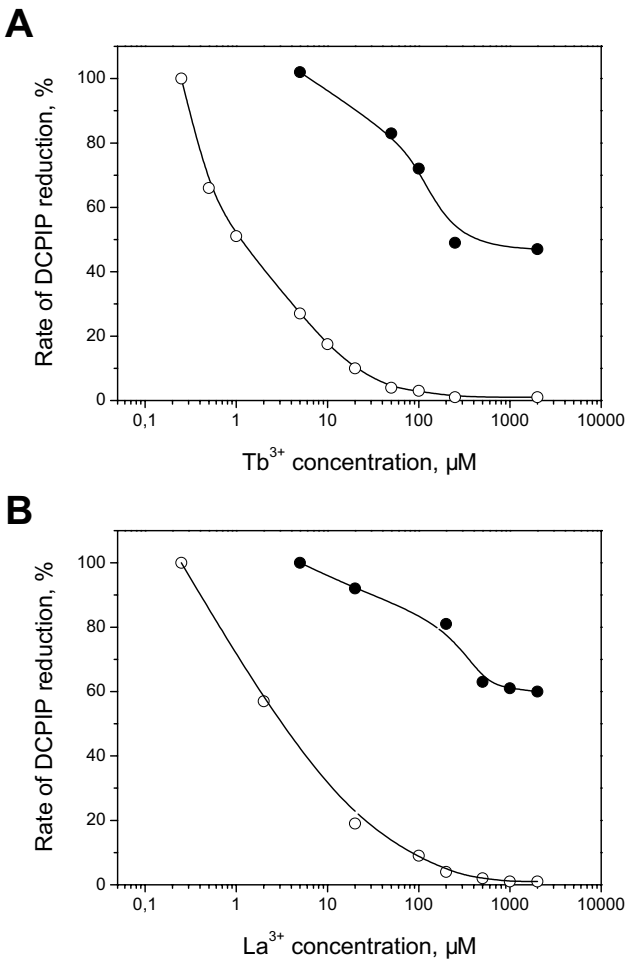

Fig. 4 Effect of different Tb^{3+} (**a**) and La^{3+} (**b**) concentrations on the light-dependent DCPIP reduction in PSII(-Mn) membranes with ($Mn^{2+} + H_2O_2$) system (open circles) or DPC (solid circles) as artificial electron donors. Concentration of PSII(-Mn) membranes in sample was 20 µg Chl/ml. 100% is the rate of DCPIP reduction (120 or 90 µmol DCPIP mg Chl^{-1} h^{-1}) by PSII(-Mn) membranes in buffer A with ($Mn^{2+} + H_2O_2$) donor system or DPC respectively. A 5 mM $Tb_2(SO_4)_3$ (10 mM Tb^{3+}) solution was prepared using buffer A. Prior to measurements, preparations were incubated with Tb^{3+} or La^{3+} for 2 min in the dark at room temperature

a new peak *K*, close to point J seen in native PSII membranes, appears and indicates Q_A reduction [42]. However, the fluorescence yield subsequently decreases after peak *K* since there is no additional electron transfer from the donor side of PSII to continue to reduce Q_A, and Q_A is rapidly oxidized by Q_B (Fig. 6a, b, curves 1). Addition of Tb^{3+} or La^{3+} cations to PSII(–Mn) membranes does not influence the shape of the FIK curve (Fig. 6a, b, curves 2), whereas in the presence of ($Mn^{2+} + H_2O_2$) electron donor FIK is significantly changed (Fig. 6a, b, curves 3). In this case, the FIK is similar to the kinetics of native PSII membranes with intact electron transport. The shape of the FIK curve in PSII(–Mn) membranes incubated with Tb^{3+} or La^{3+} before

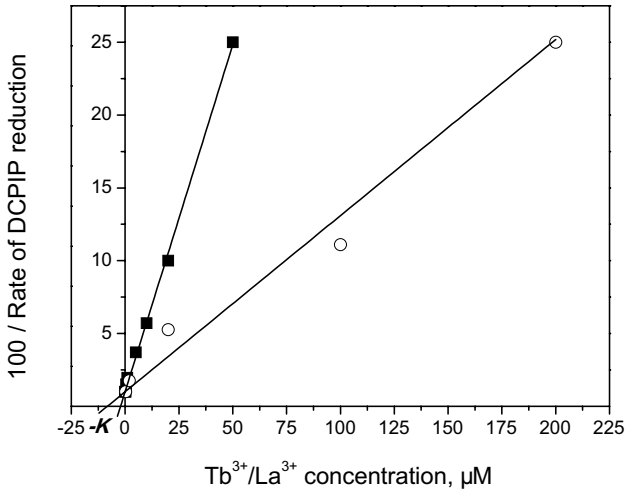

Fig. 5 Plot of the inverse of the relative initial rate of DCPIP photoreduction by (Mn^{2+} + H_2O_2) donor versus the concentration of added Tb^{3+} (filled square) or La^{3+} (unfilled circle) (Dixon plot). The results represent the values averaged over three to five measurements

addition of (Mn^{2+} + H_2O_2) donor is closer to the kinetics in PSII(–Mn) membranes without donor (Fig. 6a, b, curves 4). These results indicate that Ln^{3+} cation inhibits the Mn^{2+} oxidation at the PSII(-Mn) donor side. It is necessary to note that FIK measurement was carried out without artificial electron acceptor, allowing to eliminate possible artifacts due to reduction/oxidation of acceptor DCPIP.

Thus, the inhibition of electron transport in PSII(-Mn) membranes by lanthanoid cations has very high efficiency and K_i values of this reaction are significantly smaller than K_i value for inhibition of electron transport in PSII(-Ca) membranes (K_i is 140 μM for Tb^{3+} or 200 μM for La^{3+}) [14]. Since the inhibition of electron transport in intact PSII and PSII(-Ca) is carried out by binding of Ln^{3+} cations to Ca-binding site, we can conclude that the binding site for Tb^{3+} and La^{3+} in PSII(-Mn) membranes is not Ca-binding site. This conclusion is confirmed by the results of the next experiment where, before incubation of PSII(-Mn) membranes, we added together Tb^{3+} cations (10 μM) and Ca^{2+} cations (the indicated concentration). After incubation in dark at room temperature for 3 min, the sample was centrifuged and after washing the membranes were suspended in buffer A. Electron transport activity of treated membranes was measured using (Mn^{2+} + H_2O_2) donor and DCPIP as acceptor of electrons. The obtained results are presented in Fig. 7. These data demonstrate that Ca does not affect the interaction of Tb^{3+} with the inhibition site and provide additional evidence that Tb^{3+} binding site is different from Ca-binding site. It is necessary to note that our preliminary studies have shown that Tb^{3+} cation binds to the inhibition site very tightly and cannot be removed by centrifugation of samples.

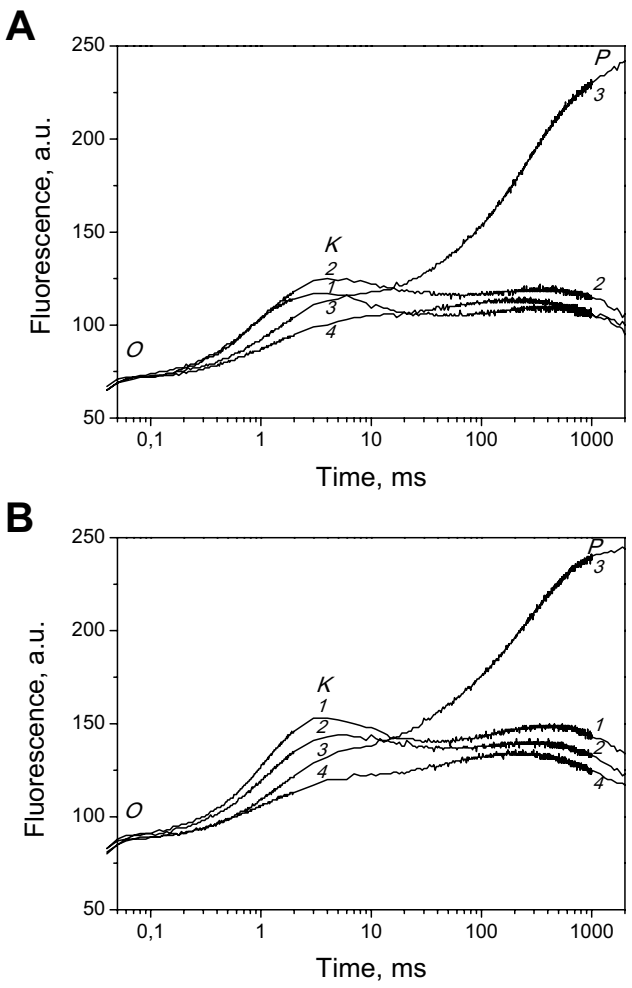

Fig. 6 Effect of Tb^{3+} (**a**) and La^{3+} (**b**) on the chlorophyll *a* fluorescence induction curves for dark adapted PSII(-Mn) membranes (20 μg Chl/ml) in buffer A. Curves 1 in **a** and **b** represent FIK in PSII(-Mn) membranes. Curves 2 in **a** and **b** represent FIK in PSII(-Mn) membranes incubated with Tb^{3+} (2 mM) or La^{3+} (2 mM), respectively, for 2 min at room temperature in dark before measurement. Curves 3 in **a** and **b**: FIK in PSII(-Mn) membranes with exogenous electron donor (Mn^{2+} + H_2O_2) (2 μM and 3 mM respectively). Curves 4 in **a** and **b**: FIK in PSII(-Mn) membranes after incubation with Tb^{3+} (2 mM) or La^{3+} (2 mM), respectively, in the presence of exogenous electron donor (Mn^{2+} + H_2O_2) during measurement

The donation of electrons by (Mn^{2+} + H_2O_2) is realized through the HA Mn-binding site [37–40]. In the process of donation, Mn^{2+} cation binds to this site and the bound cation is oxidized by $Y_Z^{\cdot}$, then Mn^{3+} is reduced by H_2O_2. Therefore, it is reasonable to suggest that Ln^{3+} cations inhibit the Mn^{2+} oxidation by interacting with the HA site. It is known that another electron donor, DPC, also donates electrons via HA site along with donation through the low affinity site [39, 43]. DPC at 200 μM donates to both sites at the same rate, but addition of several μM $MnCl_2$ non-competitively inhibits DPC photooxidation only at the HA site [43–45]. The result is a 50% decrease in the rate of DCPIP photoreduction.

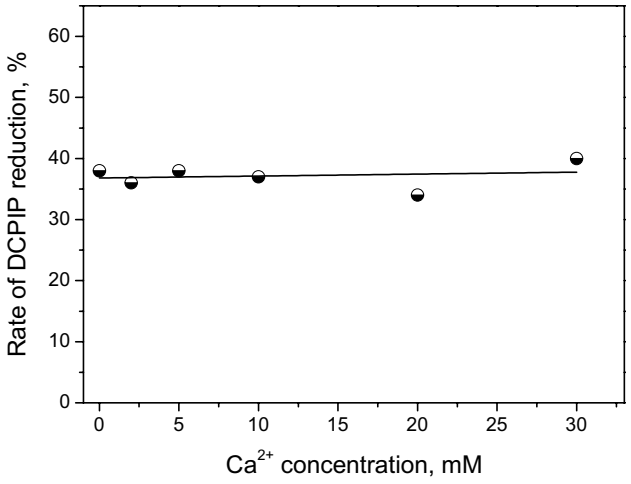

Fig. 7 Ca^{2+} effect on the inhibition of electron transport in PSII(-Mn) membranes by Tb^{3+} cations. PSII(-Mn) membranes (40 µg Chl/ml) were incubated with 10 µM Tb^{3+} and indicated Ca^{2+} concentration for 3 min in the dark at room temperature. The membranes were then pelleted by centrifugation (16100 $g \times 5$ min) at 4 °C and re-suspended in buffer A (20 µg Chl/ml). The rate of electron transport was measured as DCPIP reduction in the presence of artificial electron donor ($Mn^{2+} + H_2O_2$)

This effect has been used as the "DPC inhibition assay" for investigation of the HA site [43, 45, 46]. It was shown with using of this test that Mn^{2+} cations inhibit the process of DPC oxidation at the HA site with $K_i = 1.5$ µM [46]. The inhibition of DPC oxidation at the HA site was observed also for Fe^{2+} cations in the same range of concentration (several µM) [47]. Thus, Mn^{2+} and Fe^{2+} cations are similar to Tb^{3+} and La^{3+} cations concerning the concentration required for inhibition and K_i values.

Although in these investigations Mn^{2+} and Fe^{2+} cations were used, the inhibition of the HA site is realized by trivalent cations since the inhibition of HA site is observed only under illumination which provides oxidation of these cations [43, 47, 48]. Taking into account the fact that Ln^{3+} cations are also trivalent cations and that Mn cation bound to the HA site (Mn4) is also in trivalent state [3], we can suggest that valency can be important for interaction of metal cations with the HA site. Therefore, we studied the influence on the HA site of some other metal cations and presented the results in the Table 1. We found that trivalent cations like Cr^{3+} and Al^{3+} are less effective inhibitors than Ln^{3+}. Divalent cation Cd^{2+} is almost inactive, but at the same time apparent K_i for Zn^{2+} is about 18 µM and 33 µM for Co^{2+} [46]. Thus, the available data do not clearly support the idea of relationship between metal cation valency and its efficiency in the inhibition of the HA site.

For investigation of the possible binding of Ln^{3+} cations to the HA site, we used "DPC inhibition assay". According to this test, the inhibition of the HA site by micromolar concentration of inhibitors interacting with the HA site like Mn^{2+} [43, 45, 46] or Fe^{2+} [47, 49] is accompanied by inhibition of DPC oxidation only via the HA site. Considering that DPC donates at equal rates to HA site and low-affinity site, 100% inhibition of the HA site corresponds to a 50% decrease in the rate of DCPIP photoreduction by DPC (since after 100% inhibition of the HA site DPC continue to donate electrons via only the low affinity site). In our experiments, we found that at Ln^{3+} concentration which completely inhibits Mn^{2+} oxidation at the HA site, the rate of DCPIP reduction supported by DPC decreases by up to approximately 50% (Fig. 4). These results provide additional evidence that bound Ln^{3+} cations inhibit the HA site Mn-binding site. However, it should be noted that there is some difference in "DPC inhibition assay" for Mn^{2+}or Fe^{2+} and Tb^{3+}or La^{3+}. Inhibition of DPC and ($Mn^{2+} + H_2O_2$) donor oxidation begins in fact at the same concentration of Mn^{2+}or Fe^{2+}, whereas in the case inhibition by Tb^{3+}or La^{3+} these concentrations do not coincide (Fig. 4). Inhibition of DPC oxidation by lanthanoid cations starts when about 70–80% of the HA site is blocked by the cations. It can be suggested that probably the Mn^{3+}/Fe^{3+}

Table 1 Effect of metal ions on DCPIP reduction rate in PSII(-Mn) membranes with different electron donors

Ions	Ionic radius (Å)[a]	Concentration (µM)	DCPIP reduction rate (%)	
			Donor [$Mn^{2+} + H_2O_2$]	Donor DPC
Tb^{3+}	1.06	50	4	83
		2×10^3	0	47
La^{3+}	1.17	50	14	87
		2×10^3	0	60
Fe^{3+}[b]	0.79	5	5	40[c]
Mn^{3+}[d]	0.79	5	n.d.	50[c]
Cr^{3+}	0.76	50	19	71
		2×10^3	2	52
Al^{3+}	0.68	50	24	77
		2×10^3	27	81
Cd^{2+}	0.97	50	52	85
		2×10^3	10	74

Prior to measurements, preparations were incubated with ions for 2 min in the dark and at room temperature

[a]Data from [53]

[b]Fe^{3+} can bind to the HA site of PSII(-Mn) membranes only during the process of light-dependent oxidation of added Fe^{2+} cations at the HA site [47]. Fe^{3+} cations cannot be dissolved in buffer A (pH 6.5) due to the formation of insoluble $Fe(OH)_3$. However, Fe^{3+} cations can be stabilized by sucrose [47], but in this case iron cations form nanoparticles surrounded by sucrose shell and HA site cannot extract Fe^{3+} cations from these particles [54]

[c]Data from [47]

[d]Mn^{3+} was generated during oxidation of Mn^{2+} at the HA site under illumination

binding site partially does not coincide with the binding site for Tb^{3+}/La^{3+}.

Used in our study, the OEC-depleted PSII membranes are interesting objects for investigation of photosynthesis mechanisms (for example, for the study of one of the most important processes in photosynthesis—photoactivation). Recently, Zouni group [5] for the first time obtained the structure of PSII without Mn_4CaO_5 cluster (at 2.55 Å resolution) using *T. elongatus* PSII crystals. Unexpectedly, they found that extraction of Mn cluster is not accompanied by rearrangement of the metal-coordinating residues, i.e., HA Mn-binding site is in starting state and ready to bind metal cation. This may be important for effective binding of Ln^{3+} cation. OEC-depleted PSII crystals are able to bind Mn ions and the initial stages of photoactivation were investigated [5]. However, low resolution (4.5 Å) does not allow yet to draw certain conclusions about the structure of the partially reconstructed cluster. In this regard, the fact that we have found the high-efficient binding of Ln^{3+} cations with the HA Mn-binding site may be of some interest. The point is that Ln^{3+} cations have very good X-ray scattering properties [50]. Taking into account the possibility of Ln^{3+} cations binding to the HA site, they can be used as probes in X-ray crystallography instead of Mn ions to increase resolution. A similar approach was successfully applied by Kawakami et al. [51], who investigated Br^- anions instead of Cl^- anions. It should also be noted that HA Mn-binding site in the apo-PSII is occupied by Mn4 in the native PSII as has been proven by Asado and Mino with the use of pulsed EPR [52]. Binding metal cation is coordinated with axial ligands D170 and E333 in the D1 polypeptide which can effectively bind Ln^{3+} cations, since it is known that lanthanides typically bind ionically via oxygen-containing sidechains [50]. Based on the above data, we propose a hypothetical model for binding the lanthanide cation to the HA Mn-binding site (Fig. 8). This model is founded on the structure of PSII(-Mn) crystals obtained by Zouni group [5] (PDB:5MX2).

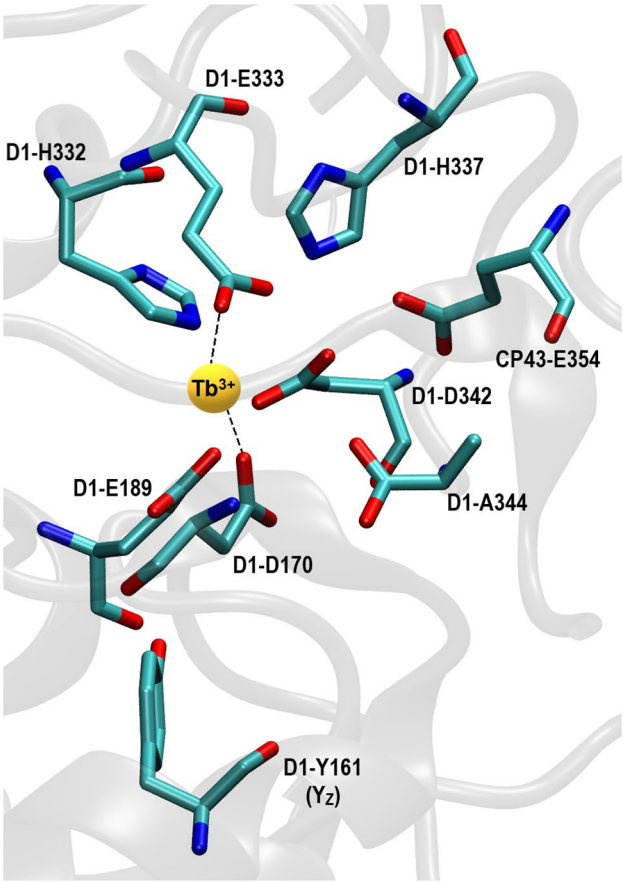

Fig. 8 Proposed binding center of Ln^{3+} ions in PSII without Mn_4CaO_5 cluster. The model is based on the structure of apo-PSII obtained by Zhang et al. [5] (PDB:5MX2). Amino acid residues forming the ligand environment of metal cluster and the residue of redox-active tyrosine Y_Z are shown. The structure is built using the VMD program (v. 1.9.3)

Conclusions

It was shown in several investigations that lanthanide ions inhibit the OEC in PSII [13, 16–18, 31, 32] and PSII(-Ca) [14] membranes. Kinetic analysis suggests that lanthanides function as a mixed-type competitor for Ca^{2+} cation included in the OEC [13]. Unexpectedly in our study, we found that lanthanide cations (Tb^{3+} and La^{3+}) strongly bind at the oxidizing side of PSII(-Mn) membranes in the dark. This binding cannot be prevented by addition of Ca^{2+} ions like the interaction of Ln^{3+} cations with PSII [13] and PSII(-Ca) [14] membranes. Bound Ln^{3+} cations inhibit the oxidation of Mn^{2+} cations of the electron donor system ($Mn^{2+} + H_2O_2$) via the HA Mn-binding site with $K_i = 2.1$ μM for Tb^{3+} ion and about 8.3 μM for La^{3+}. It should be noted that Mn^{2+} cations inhibit the DPC oxidation via the HA site with similar $K_i = 1.5$ μM [46]. Inhibition of electron donation by ($Mn^{2+} + H_2O_2$) donor is accompanied by inhibition of DPC oxidation up to 50%. These results indicate that Ln^{3+} cations bind directly or close to the HA Mn-binding site in PSII(-Mn) membranes. Taking into account the fact that Mn^{2+} and Fe^{2+} cations bind to HA site as trivalent cations after light-induced oxidation and that Mn cation bound to the HA site (Mn4) is also in trivalent state, we can suggest that valency may be important for interaction of Ln^{3+} with the HA site.

Acknowledgements We are grateful to Dr. S. Vassiliev (University of New Brunswick, Canada) for technical comments and editorial advice.

Compliance with ethical standards

Conflict of interest The authors declare that they have no conflicts of interest.

References

1. Umena Y, Kawakami K, Shen J-R, Kamiya N (2011) Crystal structure of oxygen-evolving photosystem II at a resolution of 1.9 Å. Nature 473:55–60. https://doi.org/10.1038/nature09913
2. Najafpour MM, Renger G, Hołyńska M, Moghaddam AN, Aro EM, Carpentier R, Nishihara H, Eaton-Rye JJ, Shen J-R, Allakhverdiev SI (2016) Manganese compounds as water-oxidizing catalysts: from the natural water-oxidizing complex to nanosized manganese oxide structures. Chem Rev 116:2886–2936. https://doi.org/10.1021/acs.chemrev.5b00340
3. Suga M, Akita F, Hirata K, Ueno G, Murakami H, Nakajima Y, Shimizu T, Yamashita K, Yamamoto M, Ago H, Shen J-R (2015) Native structure of photosystem II at 1.95 Å resolution viewed by femtosecond X-ray pulses. Nature 517:99–103. https://doi.org/10.1038/nature13991
4. Young ID, Ibrahim M, Chatterjee R, Gul S, Fuller FD, Koroidov S, Brewster AS, Tran R, Alonso-Mori R, Kroll T, Michels-Clark T, Laksmono H, Sierra RG, Stan CA, Hussein R, Zhang M, Douthit L, Kubin M, de Lichtenberg C, Pham LV, Nilsson H, Cheah MH, Shevela D, Saracini C, Bean MA, Seuffert I, Sokaras D, Weng TC, Pastor E, Weninger C, Fransson T, Lassalle L, Brauer P, Aller P, Docker PT, Andi B, Orville AM, Glownia JM, Nelson S, Sikorski M, Zhu DL, Hunter MS, Lane TJ, Aquila A, Koglin JE, Robinson J, Liang MN, Boutet S, Lyubimov AY, Uervirojnangkoorn M, Moriarty NW, Liebschner D, Afonine PV, Waterman DG, Evans G, Wernet P, Dobbek H, Weis WI, Brunger AT, Zwart PH, Adams PD, Zouni A, Messinger J, Bergmann U, Sauter NK, Kern J, Yachandra VK, Yano J (2016) Structure of photosystem II and substrate binding at room temperature. Nature 540:453–457. https://doi.org/10.1038/nature20161
5. Zhang M, Bommer M, Chatterjee R, Hussein R, Yano J, Dau H, Kern J, Dobbek H, Zouni A (2017) Structural insights into the light-driven auto-assembly process of the water-oxidizing Mn4CaO5-cluster in photosystem II. eLife 6:e26933. https://doi.org/10.7554/eLife.26933
6. Wei X, Su X, Cao P, Liu X, Chang W, Li M, Zhang X, Liu Z (2016) Structure of spinach photosystem II–LHCII supercomplex at 3.2 Å resolution. Nature 534:69–74. https://doi.org/10.1038/nature18020
7. Yocum CF (1991) Calcium activation of photosynthetic water oxidation. Biochim Biophys Acta 1059:1–15. https://doi.org/10.1016/S0005-2728(05)80182-3
8. Shamsipur M, Pashabadi A (2018) Latest advances in PSII features and mechanism of water oxidation. Coord Chem Rev 374:153–172. https://doi.org/10.1016/j.ccr.2018.07.006
9. Bang S, Lee Y-M, Hong S, Cho K-B, Nishida Yu, Seo MS, Sarangi R, Fukuzumi S, Nam W (2014) Redox-inactive metal ions modulate the reactivity and oxygen release of mononuclear non-haem iron(III)–peroxo complexes. Nat Chem 6:934–940. https://doi.org/10.1038/nchem.2055
10. McEvoy JP, Brudvig GW (2006) Water-splitting chemistry of photosystem II. Chem Rev 106(11):4455–4483. https://doi.org/10.1021/cr0204294
11. Waggoner CM, Yocum CF (1990) Calcium activated oxygen evolution. In: Baltscheffsky M (ed) Current research in photosynthesis. Springer, Dordrecht. https://doi.org/10.1007/978-94-009-0511-5_167
12. Ghanotakis DF, Babcock GT, Yocum CF (1984) Calcium reconstitutes high rates of oxygen evolution in polypeptide depleted photosystem II preparations. FEBS Lett 167:127–130. https://doi.org/10.1016/0014-5793(84)80846-7
13. Ghanotakis DF, Babcock GT, Yocum CF (1985) Structure of the oxygen-evolving complex of Photosystem II: calcium and lanthanum compete for sites on the oxidizing side of Photosystem II which control the binding of water-soluble polypeptides and regulate the activity of the manganese complex. Biochim Biophys Acta 809:173–180. https://doi.org/10.1016/0005-2728(85)90060-X
14. Ono T (2000) Effects of lanthanide substitution at Ca^{2+}-site on the properties of the oxygen evolving center of photosystem II. J Inorg Biochem 82:85–91. https://doi.org/10.1016/S0162-0134(00)00144-6
15. Kretsinger RH, Nelson DJ (1976) Calcium in biological systems. Coord Chem Rev 18:29–124. https://doi.org/10.1016/S0010-8545(00)82054-8
16. Lee C-I, Lakshmi KV, Brudvig GW (2007) Probing the functional role of Ca^{2+} in the oxygen-evolving complex of photosystem II by metal ion inhibition. Biochemistry 46:3211–3223. https://doi.org/10.1021/bi062033i
17. Bakou A, Ghanotakis DF (1993) Substitution of lanthanides at the calcium site(s) in photosystem II affects electron transport from tyrosine Z to $P680^{+}$. Biochim Biophys Acta 1141:303–308. https://doi.org/10.1016/0005-2728(93)90057-M
18. Loktyushkin AV, Lovyagina ER, Semin BK (2019) Interaction of terbium cations with the donor side of photosystem II in higher plants. Moscow Univ Biol Sci Bull 74:81–85. https://doi.org/10.3103/S009639251902007X
19. Ghanotakis DF, Babcock GT (1983) Hydroxylamine as an inhibitor between Z and P680 in photosystem II. FEBS Lett 153:231–234. https://doi.org/10.1016/0014-5793(83)80154-9
20. Dunahay TG, Staechelin LA, Seibert M, Ogilvie PD, Berg SP (1984) Structural biochemical and biophysical characterization of four oxygen-evolving photosystem 2 preparations from spinach. Biochim Biophys Acta 764:179–193. https://doi.org/10.1016/0005-2728(84)90027-6
21. Porra RJ, Tompson WA, Kriedemann PE (1989) Determination of accurate extinction coefficients and simultaneous-equations for assaying chlorophyll *a* and chlorophyll *b* extracted with 4 different solvents—verification of the concentration of chlorophyll standards by atomic absorption spectroscopy. Biochim Biophys Acta 975:384–394. https://doi.org/10.1016/S0005-2728(89)80347-0
22. Ono T, Inoue Y (1990) Abnormal redox reactions in photosynthetic O_2-evolving centers in NaCl/EDTA-washed PS II. A dark-stable EPR multiline signal and an unknown positive charge accumulator. Biochim Biophys Acta 1020:269–277. https://doi.org/10.1016/0005-2728(90)90157-Y
23. Boussac A, Zimmermann J-L, Rutherford AW (1990) Factors influencing the formation of modified S2 EPR signal and the S3 EPR signal in Ca^{2+}-depleted photosystem II. FEBS Lett 277:69–74. https://doi.org/10.1016/0014-5793(90)80811-V
24. Semin BK, Davletshina LN, Ivanov II, Rubin AB, Seibert M (2008) Decoupling of the processes of molecular oxygen synthesis and electron transport in Ca^{2+}-depleted PSII membranes. Photosynth Res 98:235–249. https://doi.org/10.1007/s11120-008-9347-5
25. Armstrong JM (1964) The molar extinction coefficient of 2,6-dichlorophenol indophenol. Biochim Biophys Acta 86(1):194–197. https://doi.org/10.1016/0304-4165(64)90180-1
26. Semin BK, Seibert M (2009) A simple colorimetric determination of the manganese content in photosynthetic membranes. Photosynth Res 100:45–48. https://doi.org/10.1007/s11120-009-9421-7
27. Semin BK, Davletshina LN, Ivanov II, Seibert M, Rubin AB (2012) Rapid degradation of the tetrameric Mn cluster in iluminated, PsbO-depleted photosystem II preparations. Biochemistry (Moscow) 77:152–156. https://doi.org/10.1134/S0006297912020058
28. Serrat FB (1998) 3,3′,5,5′-Tetramethylbenzidme for the colorimetric determination of manganese in water. Microchim Acta 129:77–80. https://doi.org/10.1007/BF01246852

29. Lovyagina ER, Semin BK (2016) Mechanism of inhibition and decoupling of oxygen evolution from electron transfer in photosystem II by fluoride, ammonia and acetate. J Photochem Photobiol B 158:145–153. https://doi.org/10.1016/j.jphotobiol.2016.02.031
30. Lovyagina ER, Belevich NP, Semin BK (2016) Inhibition of photosystem II electron transport chain by ammonia and "decoupling effect". Modern trends in biological physics and chemistry (BPPC) 1:95−98. https://pureportal.spbu.ru/files/9280949/Proceedings_BPPC_2016_Vol_1.pdf#page=96
31. Bakou A, Buser C, Dandulakis G, Brudvig G, Ghanotakis DF (1992) Calcium binding site(s) of photosystem II as probed by lanthanides. Biochim Biophys Acta 1099:131–136. https://doi.org/10.1016/0005-2728(92)90209-K
32. Riggs-Gelasco PJ, Mei R, Ghanotakis DF, Yocum CF, Penner-Hahn JE (1996) X-ray absorption spectroscopy of calcium-substituted derivatives of the oxygen-evolving complex of photosystem II. J Am Chem Soc 118:2400–2410. https://doi.org/10.1021/ja9504505
33. Semin BK, Davletshina LN, Timofeev KN, Ivanov II, Rubin AB, Seibert M (2013) Production of reactive oxygen species in decoupled, Ca^{2+}-depleted PSII and their use in assigning a function to chloride on both sides of PSII. Photosynth Res 117:385–399. https://doi.org/10.1007/s11120-013-9870-x
34. Ghanotakis DF, Topper JN, Youcum CF (1984) Structural organization of the oxidizing side of photosystem II. Exogenous reductants reduce and destroy the Mn-complex in photosystems II membranes depleted of the 17 and 23 kDa polypeptides. Biochim Biophys Acta 767(3):524−531. https://doi.org/https://doi.org/10.1016/0005-2728(84)90051-3
35. Semin BK, Seibert M (2016) Substituting Fe for two of the four Mn ions in photosystem II—effects on water-oxidation. J Bioenerg Biomembr 48:227–240. https://doi.org/10.1007/s10863-016-9651-2
36. Segel IW (1993) Enzyme kinetics behavior and analysis of rapid equilibrium and steady-state enzyme systems. Wiley, New York
37. Inoue H, Wada T (1987) Requirement of manganese for electron donation of hydrogen peroxide in Photosystem II reaction center complex. Plant Cell Physiol 28:767–773. https://doi.org/10.1093/oxfordjournals.pcp.a077357
38. Boussac A, Picaud M, Etienne A-L (1986) Effect of potassium iridic chloride on the electron donation by Mn^{2+} to photosystem II particles. Photobiochem Photobiophys 10:201–211
39. Semin BK, Davletschina LN, Aleksandrov AYu, Lanchinskaya VYu, Novakova AA, Ivanov II (2004) pH-dependence of iron binding to the donor side of photosystem II. Biochemistry (Moscow) 69:410–419. https://doi.org/10.1023/B:BIRY.0000022066.38297.8a
40. Ono T-A, Mino H (1999) Unique binding site for Mn^{2+} ion responsible for reducing an oxidized Y_Z tyrosine in manganese-depleted photosystem II membranes. Biochemistry 38:8778–8785. https://doi.org/10.1021/bi982949s
41. Pospíšil P, Dau H (2000) Chlorophyll fluorescence transients of photosystem II membrane particles as a tool for studying photosynthetic oxygen evolution. Photosynth Res 65:41–52. https://doi.org/10.1023/A:1006469809812
42. Strasser BJ (1997) Donor side capacity of photosystem II probed by chlorophyll *a* fluorescence transients. Photosynth Res 52:147–155. https://doi.org/10.1023/A:1005896029778
43. Hsu B-D, Lee J-Y, Pan R-L (1987) The high-affinity binding site for manganese on the oxidizing side of Photosystem II. Biochim Biophys Acta 890:89–96. https://doi.org/10.1016/0005-2728(87)90072-7
44. Preston C, Seibert M (1991) The carboxyl modifier 1-ethyl-3-[3-(dimethylamino) propyl] carbodiimide (EDC) inhibits half of the high-affinity manganese-binding site in photosystem II membrane fragments. Biochemistry 30:9615–9624. https://doi.org/10.1021/bi00104a008
45. Seibert M, Tamura N, Inoue Y (1989) Lack of photoactivation capacity in *Scenedesmus obliquus* LF-1 results from loss of half the high-affinity manganese-binding site: relationship to the unprocessed D1 protein. Biochim Biophys Acta 974:185–191. https://doi.org/10.1016/S0005-2728(89)80371-8
46. Ghirardi ML, Lutton TW, Seibert M (1996) Interactions between diphenylcarbazide, zinc, cobalt, and manganese on the oxidizing side of photosystem II. Biochemistry 35:1820–1828. https://doi.org/10.1021/bi951657d
47. Semin BK, Ivanov II, Rubin AB, Parak F (1995) High-specific binding of Fe(II) at the Mn-binding site in Mn-depleted PSII membranes from spinach. FEBS Lett 375:223–226. https://doi.org/10.1016/0014-5793(95)01215-Z
48. Hoganson CW, Ghanotakis DF, Babcock GT, Yocum CF (1989) Mn^{2+} reduces Y^+ in manganese-depleted photosystem II preparations. Photosynth Res 22:285–293. https://doi.org/10.1007/BF00048306
49. Semin BK, Ghirardi ML, Seibert M (2002) Blocking of electron donation by Mn(II) to $Y_Z^{\bullet}$ following incubation of Mn-depleted photosystem II membranes with Fe(II) in the light. Biochemistry 41:5854–5864. https://doi.org/10.1021/bi0200054
50. Boggon TJ, Shapiro L (2000) Screening for phasing atoms in protein crystallography. Structure 8:R143–R149. https://doi.org/10.1016/s0969-2126(00)00168-4
51. Kawakami K, Umena Y, Kamiya N, Shen J-R (2009) Location of chloride and its possible functions in oxygen-evolving photosystem II revealed by X-ray crystallography. PNAS 106:8567–8572. https://doi.org/10.1073/pnas.0812797106
52. Asada M, Mino H (2015) Location of the high-affinity Mn^{2+} site in photosystem II detected by PELDOR. J Phys Chem B 119:10139–10144. https://doi.org/10.1021/acs.jpcb.5b03994
53. Shannon RD (1976) Revised effective ionic radii and systematic studies of interatomic distances in halides and chalcogenides. Acta Cryst A32:751–767. https://doi.org/10.1107/S0567739476001551
54. Semin BK, Davletshina LN, Rubin AB (2019) Effect of sucrose-bound polynuclear iron oxyhydroxide nanoparticles on the efficiency of electron transport in the photosystem II membranes. Photosynth Res 142:57–67. https://doi.org/10.1007/s11120-019-00647-4